Arabian Journal of Chemistry (2019) **12**, 621–632

King Saud University

Arabian Journal of Chemistry

www.ksu.edu.sa
www.sciencedirect.com

ORIGINAL ARTICLE

Explosives properties of high energetic trinitrophenyl nitramide molecules: A DFT and AIM analysis

V. Anbu [a,*], K.A. Vijayalakshmi [b,*], R. Karunathan [c], A. David Stephen [d], P.V. Nidhin [d]

[a] *Research & Development Centre, Bharathiar University, Coimbatore 641 046, India*
[b] *Department of Physics, Sri Vasavi College, Erode 638 316, India*
[c] *Department of Physics, Dr. NGP Arts & Science College, Coimbatore 641 048, India*
[d] *Department of Physics, Sri Shakthi Institute of Engineering and Technology, Coimbatore 641 062, India*

Received 9 July 2016; revised 25 September 2016; accepted 27 September 2016
Available online 5 October 2016

KEYWORDS

TNPN;
AIM;
Impact sensitivity;
ESP

Abstract The high level density functional theory, B3LYP, was proposed for the derivatives of energetic molecule Trinitrophenyl Nitramide [TNPN]: MTNPN, ETNPN and NETNPN respectively, in order to understand its explosive characteristics. The geometrical analysis has been studied from both the polarized, 6-311G** and augmented, aug-cc-pVDZ basis sets, and found consistency between the structural parameters. The bond strength of each molecule has been characterized from Bader's AIM analysis, thereby correlating the bond topological properties with the impact sensitivity, which predicts that C—NO_2 bonds were the weakest and found more sensitive among the rest of the bonds in all three molecules. The impact sensitivity of the molecules was measured in terms of $\Delta E_{LUMO\text{-}HOMO}$, OB_{100}, Q_{NO2}, h_{50}% and V_{mid}, revealed the high sensitive nature of NETNPN toward the external shock. The reaction surface of all the three molecules has been located from the isosurface of electrostatic potential.

1. Introduction

The most important criteria for a high energy density material to be a good explosive candidate depend on its sensitivity toward the external shocks. The ability of the high energetic materials to release high amount of energy should be controlled by reducing the sensitivity, mainly for military purposes, in order to prevent accidental explosions and human hazards, while treating experimentally. Compelling efforts have been reported in designing new energetic with low shock sensitivity by analyzing a large number of nitro derivatives (Agarwal, 2011; Klapötke, 2011; Butcher et al., 2003). As the sensitivity of these mate-

* Corresponding authors.
E-mail addresses: v.anbuvee@gmail.com (V. Anbu), kavijayalakshmi@yahoo.co.in (K.A. Vijayalakshmi).
Peer review under responsibility of King Saud University.

Production and hosting by Elsevier

http://dx.doi.org/10.1016/j.arabjc.2016.09.023
1878-5352

rials relies on their chemical nature mainly bond electron density $\rho(r)$, Laplacian of electron density $\nabla^2\rho(r)$, energy density distribution and electrostatic potential (ESP) of the molecule, quantum chemical calculations have been implemented for the investigation, from past few decades to generate and design suitable explosive molecules which can alter the existing system of explosives and propellants. Reduction in the sensitivity by analyzing the chemical nature of the explosive compounds through quantum computational chemistry contributes to the development of new materials that combine high performance and low impact sensitivity (Murray et al., 1995). The Laplacian of the electron density is more significant in determining the bond strength and their local energy density, thereby correlating with the impact sensitivity. There are many reports suggesting the relation between the bond strength and the impact sensitivity. In the report by Politzer et al. (1991), the impact sensitivity of seven nitramine and five nitroaliphatic explosives was expressed as a function of the molar mass and the reciprocals of the experimental and computed lengths of the N—NO_2 and C—NO_2 bonds. In other approach by Zhang et al., they assessed the sensitivity of explosives compounds by means of BLYP/DNP optimized geometries and Mulliken charges of the nitro groups (Q_{NO2}) (Zhang, 2008, 2009) through which they established a correlation between sensitivity and electronic structures of 38 nitroaromatics. According to the authors, the greater the nitro group (Q_{NO2}) negative charges, the lower their electron-attraction ability, the more stable is the nitro compound. Recently, Anders and Borges, 2011 published a new approach to analyze the multipoles associated with the atomic sites of 17 nitroaromatic molecules through charge density analysis implemented through a DFT one electron density matrix. The vital results of the research suggested that explosives with large delocalized electron densities in the aromatic ring of the component molecule, expressed by large quadrupole values on the ring carbon atoms exhibit the nature of a insensitive high energy material. From the influence of the previous studies and reports, the aim of the current paper is to interpret the charge density and the topological properties of three booster explosives of trinitrophenyl nitramide molecules (TNPN); N-methyl-N-(2,4,6-trinitrophenyl)nitramide (MTNPN), N-ethyl-N-(2,4,6-trinitrophenyl)nitramide (ETNPN) and N-(2-nitroethynyl)-N-(2,4,6-trinitrophenyl)nitramide (NETNPN) (Fig. 1). These molecules are sensitive secondary high explosives used as a booster, a small charge placed next to the detonator in order to propagate detonation into the main explosive charge (Cooper, 1996). The Quantum theory of Atoms in Molecules (QTAIM) (Bader, 1990) analyzes the critical points of the molecule where the first derivative of the electron density depreciates to zero from the calculated electron density $\rho(r)$. The Eigen values deciding the critical points were also calculated to find the type of critical point formed in the concerned molecule. Depending on the values of the three eigen values (λ_1, λ_2, and λ_3) and the eigen vectors which justify the direction of the curvature, the molecules were found to be having BCP designated as (3, −1). From the location of the BCP and the electron density associated with the system, the strength and the nature of the chemical bonds can be studied with accuracy, thereby evaluating the sensitivity of the system toward the external shocks.

2. Methods and computational details

As far as the molecules under investigations are concerned, increased number of rotational bonds prevailed within the molecules exhibits a large number of conformational geometries in the room temperature. In order to find the stable conformers, the systematic rotor search (SRS) algorithm with MMFF94 force field was implemented (Hanwell et al., 2012). The local minima for each molecules under investigation generated from MMFF94 force field and B3LYP/aug-cc-pVDZ basis set method are given in Table 1. To carry out the charge density analysis and to derive the electrostatic and explosives properties, the stable confirmers were optimized using DFT (Perdew, 1986) method utilizing the Becke's three parameter exchange functional combined with the correlation functional (B3LYP) with the basis sets 6-311G** and aug-cc-pVDZ in gas phase, which reports the successful accurate prediction of the inter and intra molecular interactions and topology of the molecules. Many studies have been reported the accuracy and reliability of DFT optimization with the experimental characteristics of the molecules (Brovarets and Hovorun, 2013).

The complete calculations initiated from the local minima obtained for each molecules under investigation were carried out using Gaussian09 package (Frish et al., 2005). Both the level calculations were converged at the threshold limits 0.000450 and 0.001800 au for the maximum force and displacement respectively to validate the optimizations within the thermodynamic stability of the isolated system. Further, the topological properties of the charge density distribution have been carried out from the wave function obtained from DFT calculation using Bader's theory of atoms in molecules (Bader, 1990), which is incorporated in AIMPAC software (Biegler-könig et al., 1982). The contour plot of deformation electron density and the Laplacian of electron density are visualized with XDGRAPH module incorporated in XD package (Koritsanszky et al., 2007). The electrostatic potential surfaces with positive and negative regions were mapped with MOLISO software (Hübschle and Luger, 2006).

The electronic information in the bonding region has been established from the electron density $\rho_{bcp}(r)$, Laplacian of electron density $\nabla^2\rho_{bcp}(r)$, and other characteristics of bond critical point. The atomic interaction i.e. bond path was contributed from the pair of gradient lines in $\nabla\rho(r)$ field originated at the critical point and terminated at the two neighboring nucleus. The corresponding bcp was represented as (3, −1) which is characterized from three nonzero eigen values of Hessian matrix, λ_1, λ_2 and λ_3 respectively. The sign of the

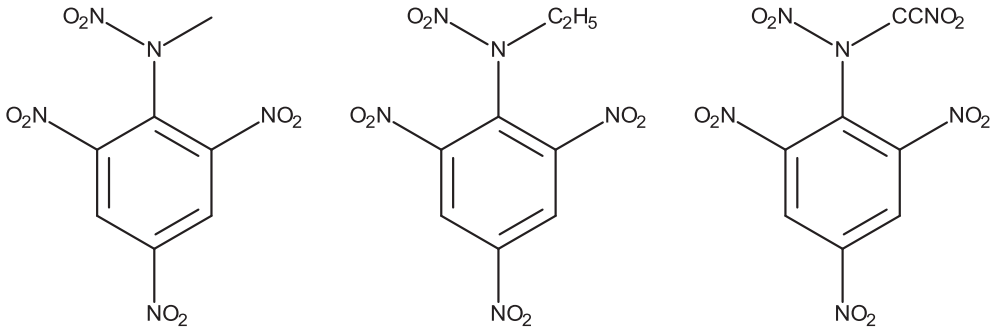

Figure 1 Chemical structure of MTNPN, ETNPN and NETNPN molecules.

Table 1 Energies (kJ/mol) of the stable confirmers of TNPN molecules.

Molecule	Energy (kJ/mol)	
	MMFF94	B3LYP
MTNPN	349.1	−3006308.52
ETNPN	332.91	−3109538.50
NETNPN	−37.09	−3639909.88

Laplacian value was reflected from the λ_i values. For open shell interaction [$\nabla^2\rho_{bcp}(r) < 0$], the electron is locally concentrated around bcp, whereas the case is $\nabla^2\rho_{bcp}(r) > 0$ for the closed shell interactions in which the charges were concentrated in each of the atomic basin. Further, the total energy density distribution [$H(r)$] has also been analyzed, which was given as

$$H(r) = G(r) + V(r) \quad (1)$$

where $G(r)$ and $V(r)$ are the kinetic and potential energy densities in the bonding region. As $V(r)$ is negative, it indicates the charge concentration, whereas the charge depletion in the bonding region is from the positive $H(r)$.

3. Results and discussion

3.1. Structural aspects and heat of formation

The TNPA molecules were optimized at a higher DFT level method [B3LYP] using both polarized and augmented basis sets of 6-311G** and cc/pVDz respectively (Fig. 2) to analyze their topological properties which decide the sensitivity toward external shock. The C—N bonds in the aromatic rings were found to be exhibiting an average bond lengths of ~1.48 Å without notable variations in polarized and augmented basis operations. The bond lengths of the C—C bonds in the aromatic ring for each molecule were found to be ~1.39 Å, with the shortest bond appeared between C(2)—C(3) atoms of the ring; notably, the C—C bond lengths are found to be well in agreement with the standard C—C bonds (Lide, 1967). A feasible impact was notified for the N(16)—N(17) and C(6)—N(16) bonds with corresponding variation of ~0.1 Å and ~0.2 Å for the augmented and polarized basis set operation. Further analysis on N—O bonds showed that the interaction was consistently exhibiting a bond lengths of ~1.2 Å in all TNPN molecules without much variations, indicates the stability of the bond, with N(17)—O(19) being the shortest and N(22)—O(24) being the longest bond with 1.20 Å and 1.23 Å respectively for NETNPN. The results of the structural studies thus justified the invariance of the bond lengths associated with the molecules with different basis set operations.

As the bond length analysis exposed the unvarying nature of the bondlengths, researchers aimed to study the deviation and the distortion caused to the molecules due the presence of the nitro functional groups. The molecules, MTNPN, ETNPN and NETNPN were subjected for geometrical analysis and the results were tabulated (Table 2) and interpreted as well. The studies showed that the bond angle of C—C—C atoms of the aromatic ring was found to be standard (Sutton, 1965), exhibiting ~120°, with an observed exception for the C(1)—C(6)—C(5) bond angle of ETNPN and NETNPN. The concerned bond angle exhibited a lower value of 116.1° and 117.2° respectively for each structure. The orientation of nitrogen atoms attached to the aromatic ring also revealed the bond angle ranging from 115° to 121°, with C(4)—C(5)—N(10) making a least angle of 115° for MTNPN. Further studies over the nitro groups in the non-ring region of the molecules showed N(17) atoms are deviated from the corresponding terminal carbon atoms (C(20), C(21) and C(20) for MTNPN, ETNPN and NETNPN respectively) with a variation from 117° to 119°, a maximum deviation of 119.19° observed for N(17)—N(16)—C(20) of NETNPN, which might be due to the extra NO_2 group attached to the C(21) atom. The distortions of the bonds were thoroughly studied by resolving the torsion angles of each system of molecule in detail. The studies to investigate the torsional distortions of the molecules exposed that the nitro group attached

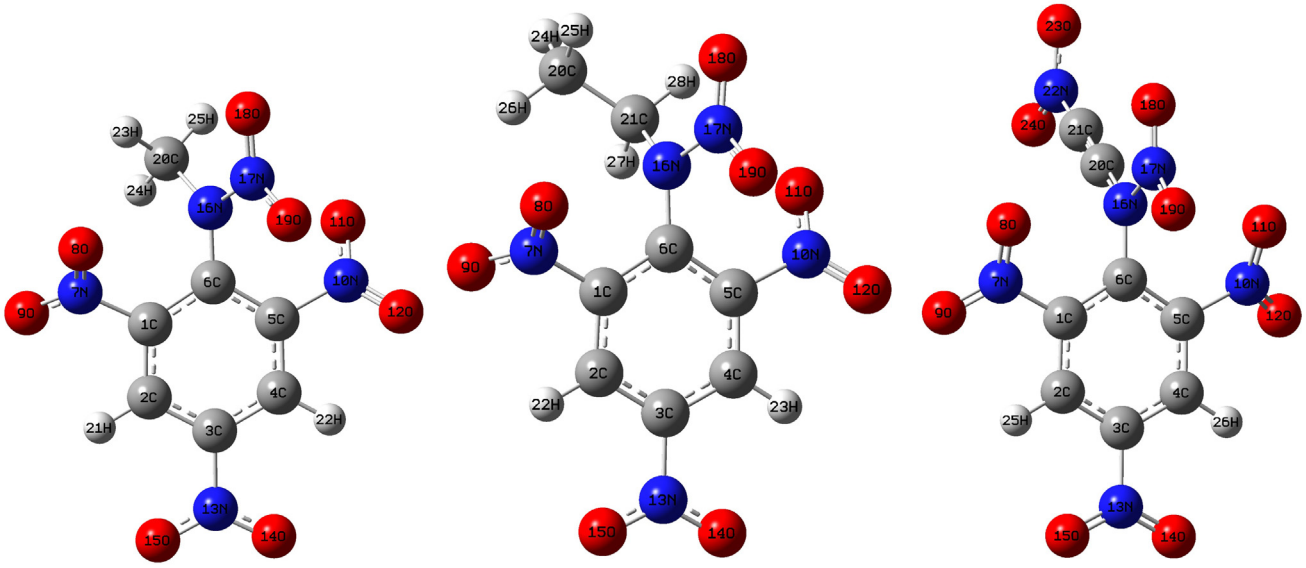

Figure 2 Optimized structures of MTNPN, ETNPN and NETNPN molecules at B3LYP/aug-cc-pVDZ.

Table 2 Selected geometrical parameters (Å, °) of TNPN molecules optimized at B3LYP/aug-cc-pVDZ.

	MTNPN	ETNPN	NETNPN
C(1)—C(2)	1.392	1.391	1.391
C(1)—C(6)	1.409	1.404	1.407
C(2)—C(3)	1.389	1.389	1.390
C(3)—C(4)	1.392	1.392	1.390
C(4)—C(5)	1.389	1.390	1.391
C(5)—C(6)	1.411	1.411	1.407
C(1)—N(7)	1.484	1.482	1.488
C(3)—N(13)	1.481	1.482	1.486
C(5)—N(10)	1.484	1.483	1.488
C(6)—N(16)	1.406	1.417	1.423
N(7)—O(8)	1.224	1.221	1.223
N(7)—O(9)	1.226	1.227	1.223
N(10)—O(11)	1.226	1.226	1.223
N(10)—O(12)	1.221	1.222	1.223
N(13)—O(14)	1.225	1.225	1.224
N(13)—O(15)	1.225	1.225	1.224
N(16)—N(17)	1.389	1.390	1.484
N(17)—O(18)	1.221	1.221	1.201
N(17)—O(19)	1.228	1.229	1.209
N(16)—C(20)	1.463	1.481	1.320
C(20)—C(21)	–	1.526	1.215
C(21)—N(22)	–	–	1.386
N(22)—O(23)	–	–	1.229
N(22)—O(24)	–	–	1.232
C(2)—C(1)—N(7)	116.0	116.5	116.3
C(2)—C(3)—N(13)	119.0	118.9	118.8
C(4)—C(5)—N(10)	116.0	116.2	116.3
C(1)—C(6)—N(16)	120.8	119.7	121.3
C(6)—N(16)—N(17)	118.5	116.1	116.7
C(6)—N(16)—C(20)	124.1	122.3	123.9
N(17)—N(16)—C(20)	117.4	118.2	119.4
C(2)—C(3)—N(13)—O(14)	179.5	179.1	179.6
C(6)—C(5)—N(10)—O(11)	−35.9	−32.9	30.2
C(2)—C(1)—N(7)—O(9)	−41.1	−52.6	−28.9
C(1)—C(6)—N(16)—N(17)	122.1	116.3	92.0
C(6)—N(16)—N(17)—O(19)	−0.5	−8.9	0.0

to the C(3) atoms of each structures is in planar with the aromatic ring. It can also be found that the transposition of O(14) with respect to C(2) justifies the stability of the linkage by making a dihedral angle ~180° for each structures. Further analysis on the remaining nitro functional groups exposed the gauche position of O(11) with C(4) for the torsion angle is ~32° with concerned aromatic carbon. A slight cis conformation can be observed in NETNPN for the nitro group attached to C(1), with torsion angle of 28° [C(2)—C(1)—N(7)—O(9)]. The review of the torsion angle of the chemical bond which links the aromatic ring and phenyl substituent of the molecule via C(6)—N(16), showed that the bond is twisted to make an anticlinal conformation with the ring, thereby exhibiting the non-planar geometry of the molecule. The concerned torsion angle, C(1)—C(6)—N(16)—N(17) was found to be ranging from ~121° to ~91° corresponding to each structures, in which NETNPN makes the least bond twist of 91.9°. An individual result was observed for the cis conformation of C(6)—N(16)—C(20)—C(21) of NETNPN in which a dihedral angle difference of ~6° was observed due to the basis set effect. Apart from this observation, the investigation revealed the insignificant effect of the basis set operation over the geometrical structure of the molecules.

3.2. Electron density

AIM theory (Bader, 1990) is a pioneer tool to analyze the charge density distribution and the electrostatic properties for the gas phase molecules from quantum chemical theory. A bcp search on all bonds of the molecule has been carried out to characterize the electron density at the BCP, in which a (3, −1) type of critical point was found for all bonds of TNPN molecules from the polarized and augmented basis sets. The bond topological parameters of electron density at the critical points of each bond have been determined and are listed in Table 3. Fig. 3 shows the deformation density map of three TNPN molecules. The electron density $\rho_{bcp}(r)$ of aromatic C—C bonds of the three molecules are almost equal and the average value is ~2.11/~2.08 eÅ^{-3} in 6-311G**/aug-cc-pVDZ basis sets and this value agrees with the reported structure having similar C—C bonds (Stephen et al., 2011). Because of the phenyl substituent at C(6) atom, the $\rho_{bcp}(r)$ of C(1)—C(6) and C(5)—C(6) bonds reduced feebly [0.07 eÅ^{-3}] when compared to the rest of C_{aro}—C_{aro} bonds. Also, the maximum deformation density has been noticed for C≡C bond [~2.60 eÅ^{-3}] in NETNPN molecule among the non-ring C—C bonds of all the three analogue molecules, which reveals its triple bond nature. From the spectrum of the deformation density of all the bonds in the TNPN molecules, the charge accumulation in C—NO_2 bonds is found significantly low with an average value ~1.74 eÅ^{-3} which agrees well with the reported structures (Stephen et al., 2010). From Fig. 3, the deformation density of —NO_2 groups reveals the orientation of oxygen loan pair electrons. As expected, the maximum electron density distribution is predicted for N═O bonds of nitro groups and the values are ~3.42 and ~3.39 eÅ^{-3} from both the levels of calculations. Notably, the non-ring C—N bonds carry different densities, and among these the maximum electron density is predicted for C(20)—N(16) [~2.27 eÅ^{-3}] in NETNPN molecule when compared to the C(6)—N(16) [~1.95 eÅ^{-3}] and C(21)—N(22) [~2.10 eÅ^{-3}]. The lowest bond density was found for C_{aro}—NO_2 bonds [~1.74 eÅ^{-3}] in all the three TNPN molecules and non-ring C—N bonds [~1.63 eÅ^{-3}] in MTNPN and ETNPN molecules. The bond density for aromatic, ethyl and methyl C—H bonds is almost similar with an average value of [~1.95 eÅ^{-3}] from both the levels of calculations.

The position of bcp has been revealed from the bond path analysis of all three TNPN molecules, from which the bond charge polarization of each bonds has been calculated. Among the non-hydrogen atoms, C_{aro}—C_{aro} and N—N bonds are less polarized bonds which are confirmed from the small bcp shift of about ~1.0/~0.8 and ~0.7/~0.9 Å from both the levels of calculations. The maximum bcp shift [~10.6/~11.0 Å] from the bond midpoint has been noticed for the C—N bonds among the non-hydrogen atoms and bcp is pushed toward the respective carbon atoms. Both the levels of calculations result in the similar bcp shift for N═O bonds of about ~2.4 Å from the bond midpoint. In the whole spectrum of bond charge polarization, the C—H bonds are highly polarized due to heavy and light atom interaction.

3.3. Laplacian of electron density

The Laplacian of electron density ($\nabla^2\rho_{bcp}(r)$) at the bcp provides significant information about the charge concentration

Table 3 Bond topological properties of TNPN molecules calculated at B3LYP/aug-cc-pVDZ.

Bonds	$\rho_{bcp}(r)$	$\nabla^2\rho_{bcp}(r)$	λ_1	λ_2	λ_3	ε	$V(r)$	$G(r)$	$H(r)$	$d1$	$d2$	D	$\nabla d\%$
Ring													
C(2)—C(1)	2.09	−18.2	−15.1	−12.5	9.3	0.21	−2.65	0.69	−1.96	0.679	0.713	1.392	1.2
	2.09	−18.2	−15.1	−12.5	9.4	0.21	−2.65	0.69	−1.96	0.679	0.713	1.392	1.2
	2.09	−18.4	−15.2	−12.6	9.4	0.20	−2.66	0.69	−1.98	0.714	0.678	1.392	1.3
C(2)—C(3)	2.11	−18.7	−15.4	−12.7	9.4	0.21	−2.68	0.69	−1.99	0.683	0.706	1.389	0.8
	2.10	−18.6	−15.4	−12.7	9.4	0.21	−2.67	0.69	−1.99	0.707	0.683	1.39	0.9
	2.10	−18.7	−15.3	−12.8	9.4	0.20	−2.67	0.68	−1.99	0.682	0.708	1.39	0.9
C(3)—C(4)	2.09	−18.5	−15.2	−12.7	9.4	0.20	−2.64	0.67	−1.97	0.709	0.683	1.392	0.9
	2.09	−18.5	−15.2	−12.7	9.4	0.20	−2.65	0.68	−1.97	0.682	0.71	1.392	1.0
	2.10	−18.7	−15.3	−12.8	9.4	0.20	−2.67	0.68	−1.99	0.708	0.682	1.39	0.9
C(4)—C(5)	2.10	−18.4	−15.3	−12.5	9.4	0.22	−2.69	0.70	−1.99	0.678	0.711	1.389	1.2
	2.10	−18.4	−15.2	−12.5	9.3	0.22	−2.68	0.70	−1.98	0.678	0.712	1.39	1.2
	2.09	−18.4	−15.2	−12.6	9.4	0.20	−2.66	0.69	−1.98	0.714	0.678	1.392	1.3
C(1)—C(6)	2.03	−17.2	−15.0	−11.8	9.6	0.27	−2.50	0.65	−1.85	0.71	0.7	1.41	0.4
	2.05	−17.5	−15.2	−11.9	9.6	0.28	−2.55	0.66	−1.89	0.695	0.71	1.405	0.5
	2.04	−17.3	−15.1	−11.9	9.6	0.27	−2.51	0.65	−1.86	0.706	0.702	1.409	0.1
C(6)—C(5)	2.02	−17.2	−14.9	−11.9	9.6	0.26	−2.47	0.63	−1.84	0.704	0.708	1.413	0.1
	2.02	−17.1	−14.9	−11.8	9.6	0.26	−2.47	0.64	−1.83	0.711	0.701	1.412	0.4
	2.04	−17.3	−15.1	−11.9	9.6	0.27	−2.51	0.65	−1.86	0.702	0.706	1.409	0.1
Ring C—NO_2													
N(13)—C(3)	1.74	−15.3	−13.0	−11.7	9.4	0.11	−2.65	0.79	−1.86	0.897	0.584	1.481	10.6
	1.74	−15.2	−13.0	−11.7	9.5	0.11	−2.63	0.78	−1.85	0.897	0.585	1.482	10.5
	1.73	−15.0	−13.0	−11.8	9.7	0.10	−2.55	0.75	−1.80	0.592	0.894	1.486	10.2
N(7)—C(1)	1.74	−15.2	−12.8	−11.8	9.4	0.09	−2.61	0.78	−1.84	0.898	0.586	1.484	10.5
	1.75	−15.6	−13.0	−12.1	9.5	0.08	−2.63	0.77	−1.86	0.586	0.897	1.482	10.5
	1.73	−15.0	−13.0	−11.8	9.8	0.10	−2.51	0.73	−1.78	0.892	0.596	1.488	9.9
C(5)—N(10)	1.74	−15.3	−13.0	−12.0	9.7	0.09	−2.58	0.75	−1.83	0.59	0.894	1.484	10.2
	1.74	−15.3	−13.0	−11.9	9.6	0.10	−2.60	0.76	−1.84	0.895	0.588	1.483	10.4
	1.73	−15.0	−13.0	−11.8	9.8	0.10	−2.51	0.73	−1.78	0.596	0.892	1.488	10.0
Ring-tail C—N													
C(6)—N(16)	1.98	−21.0	−15.1	−13.8	7.8	0.09	−3.48	1.01	−2.48	0.55	0.856	1.406	10.9
	1.96	−20.1	−14.8	−13.8	8.4	0.08	−3.20	0.90	−2.31	0.567	0.851	1.418	10.0
	1.90	−19.3	−13.9	−13.3	7.9	0.05	−3.28	0.96	−2.31	0.871	0.553	1.424	11.2
Ring NO_2													
O(9)—N(7)	3.38	−25.4	−30.8	−27.7	33.2	0.11	−6.91	2.57	−4.34	0.646	0.58	1.226	2.7
	3.37	−25.2	−30.7	−27.6	33.1	0.11	−6.88	2.56	−4.32	0.58	0.647	1.227	2.7
	3.39	−25.5	−30.9	−27.9	33.2	0.11	−6.97	2.59	−4.38	0.644	0.58	1.223	2.6
N(7)—O(8)	3.39	−25.6	−30.9	−27.8	33.2	0.11	−6.95	2.58	−4.37	0.579	0.645	1.224	2.7
	3.41	−25.9	−31.2	−28.0	33.3	0.12	−7.04	2.61	−4.43	0.644	0.577	1.221	2.7
	3.39	−25.6	−30.9	−27.9	33.2	0.11	−6.96	2.58	−4.38	0.644	0.579	1.223	2.7
N(10)—O(12)	3.41	−25.9	−31.1	−28.1	33.3	0.11	−7.03	2.61	−4.42	0.578	0.644	1.221	2.7
	3.41	−25.9	−31.1	−28.0	33.3	0.11	−7.02	2.60	−4.41	0.644	0.578	1.222	2.7
	3.39	−25.5	−30.9	−27.9	33.2	0.11	−6.97	2.59	−4.38	0.58	0.644	1.223	2.6
N(10)—O(11)	3.37	−25.4	−30.8	−27.7	33.1	0.11	−6.90	2.56	−4.34	0.58	0.645	1.226	2.7
	3.37	−25.4	−30.8	−27.7	33.1	0.11	−6.88	2.55	−4.33	0.58	0.646	1.226	2.7
	3.39	−25.6	−30.9	−27.9	33.2	0.11	−6.96	2.59	−4.38	0.644	0.579	1.223	2.7
O(15)—N(13)	3.38	−25.4	−30.7	−27.8	33.1	0.10	−6.90	2.56	−4.34	0.645	0.581	1.225	2.6
	3.38	−25.5	−30.8	−27.9	33.1	0.10	−6.91	2.56	−4.35	0.58	0.645	1.225	2.7
	3.39	−25.6	−30.8	−27.9	33.2	0.10	−6.95	2.58	−4.37	0.644	0.58	1.224	2.6
N(13)—O(14)	3.38	−25.5	−30.8	−27.9	33.1	0.10	−6.92	2.57	−4.35	0.58	0.645	1.225	2.7
	3.38	−25.6	−30.8	−27.9	33.1	0.10	−6.93	2.57	−4.36	0.645	0.58	1.225	2.7
	3.39	−25.6	−30.8	−27.9	33.2	0.10	−6.95	2.58	−4.37	0.58	0.644	1.224	2.6

(*continued on next page*)

Table 3 (*continued*)

Bonds	$\rho_{bcp}(r)$	$\nabla^2\rho_{bcp}(r)$	λ_1	λ_2	λ_3	ε	$V(r)$	$G(r)$	$H(r)$	$d1$	$d2$	D	∇d%
Tail C—N													
C(20)—N(16)	1.66	−13.5	−10.5	−10.1	7.2	0.04	−3.11	1.09	−2.03	0.537	0.926	1.463	13.3
	1.60	−12.2	−10.0	−9.7	7.5	0.04	−2.80	0.98	−1.83	0.929	0.552	1.482	12.7
	2.28	−22.8	−16.4	−16.3	9.9	0.01	−6.04	2.22	−3.82	0.466	0.854	1.32	14.7
Tail N—N													
N(16)—N(17)	2.33	−15.9	−20.6	−15.8	20.6	0.30	−3.50	1.20	−2.31	0.679	0.709	1.389	1.1
	2.33	−15.8	−20.5	−15.8	20.5	0.30	−3.49	1.19	−2.30	0.713	0.677	1.391	1.3
	1.90	−10.1	−16.0	−13.1	19.0	0.23	−2.59	0.94	−1.65	0.746	0.738	1.484	0.3
Tail NO_2													
N(17)—O(18)	3.41	−24.8	−30.6	−27.8	33.5	0.10	−7.00	2.63	−4.37	0.585	0.636	1.221	2.1
	3.41	−24.9	−30.6	−27.8	33.5	0.10	−7.01	2.63	−4.38	0.585	0.636	1.221	2.1
	3.56	−26.9	−31.8	−29.1	34.0	0.09	−7.60	2.86	−4.74	0.629	0.573	1.201	2.3
N(17)—O(19)	3.35	−23.9	−30.0	−27.2	33.3	0.10	−6.81	2.57	−4.24	0.59	0.638	1.228	2.0
	3.35	−23.9	−30.0	−27.2	33.2	0.10	−6.79	2.56	−4.23	0.639	0.59	1.229	2.0
	3.50	−26.1	−31.3	−28.6	33.7	0.10	−7.37	2.77	−4.60	0.577	0.632	1.209	2.3
Ring C—H													
H(21)—C(2)	1.92	−27.5	−18.4	−18.4	9.3	0.00	−2.33	0.20	−2.13	0.332	0.723	1.055	18.5
	1.92	−27.4	−18.4	−18.3	9.2	0.00	−2.33	0.20	−2.12	0.722	0.334	1.056	18.4
	1.93	−27.9	−18.6	−18.5	9.3	0.00	−2.34	0.20	−2.15	0.327	0.728	1.055	19.0
C(4)—H(22)	1.92	−27.6	−18.5	−18.4	9.3	0.00	−2.34	0.20	−2.14	0.724	0.331	1.055	18.6
	1.92	−27.6	−18.5	−18.4	9.3	0.00	−2.34	0.20	−2.14	0.33	0.725	1.055	18.7
	1.93	−27.9	−18.6	−18.5	9.3	0.00	−2.34	0.20	−2.15	0.728	0.327	1.055	
Methyl C—H													
H(23)—C(20)	1.90	−25.6	−17.8	−17.2	9.4	0.03	−2.28	0.24	−2.04	0.358	0.708	1.066	16.4
	1.83	−22.9	−16.1	−16.0	9.2	0.01	−2.20	0.30	−1.90	0.689	0.382	1.071	14.3
	–	–	–	–	–	–	–	–	–	–	–	–	–
H(24)—C(20)	1.88	−24.8	−17.4	−16.8	9.4	0.03	−2.27	0.27	−2.01	0.369	0.697	1.066	15.4
	1.86	−24.0	−16.7	−16.5	9.2	0.01	−2.24	0.28	−1.96	0.372	0.695	1.067	15.1
	–	–	–	–	–	–	–	–	–	–	–	–	–
C(20)—H(25)	1.89	−25.4	−17.7	−17.1	9.4	0.03	−2.27	0.24	−2.02	0.709	0.358	1.067	16.4
	1.84	−23.2	−16.3	−16.2	9.3	0.01	−2.22	0.30	−1.92	0.688	0.381	1.069	14.4
	–	–	–	–	–	–	–	–	–	–	–	–	–

and depletion of chemical bonds, which allows predicting the strength of bonds and the type of interaction between the atoms in molecule (Bader et al., 1981). Here, the Laplacian of electron density and the energy density distribution of each bonds of the TNPN have been calculated for the three analogue molecules. Fig. 4 shows the Laplacian of electron density distribution of analogue molecules. The uniform charge density distribution in the contours of C_{aro}—C_{aro} bonds reveals their covalent bonding interactions and the $\nabla^2\rho_{bcp}(r)$ values at bcp's are almost equal: ∼−21/∼−18 eÅ^{-5}. The effect of maximum electron density of C≡C bond in NETNPN molecule attributes that the bond charges are highly concentrated [−25.1/−20.8 eÅ^{-5}]. Notably, its corresponding total bond energy density $H(r)$ is also high and the average value is −3.51 HÅ^{-3}. Both the levels of DFT calculations predict that the charges in C—NO_2 bonds are highly depleted and their $\nabla^2\rho_{bcp}(r)$ values are ∼−16.1 and ∼−15.2 eÅ^{-5} respectively. This was further confirmed from the lowest bond energy density −1.83 HÅ^{-3}. Next to C—NO_2 bonds, the bond charges are found to be highly depleted for N—N [N(16)—N(17)] bonds in MTNPN [−13/−15.9 eÅ^{-5}], ETNPN [−13/−15.8 eÅ^{-5}] and NETNPN [−5.9/−10.1 eÅ^{-5}] molecules and C—N [C(20)—N(16)] bonds in MTNPN [−13.3/−13.5 eÅ^{-5}] and ETNPN [−12.7/−12.2 eÅ^{-5}] molecules, whereas in NETNPN molecule, the charges are concentrated [−19.3/−22.8 eÅ^{-5}] in C(20)—N(16) bond. This unusual charge concentration may be due to the —$CCNO_2$ attachment with C(20) atom of NETNPN molecule. Invariably, the Laplacian values for all N═O bonds in NO_2 groups are found to be highly negative [∼−25.9/∼−25.6 eÅ^{-5}], which reveals their concentration of bond charges at the bcp. It was further empathized from the high potential energy $V(r)$ in the bonding region [∼−7.03/∼−6.95 HÅ^{-3}]. Relatively, the negative Laplacian values for aromatic C—H bonds [∼−24.8/∼−27.7 eÅ^{-5}] are feebly increased in comparison with that of methyl [∼−22.8/∼−24.3 eÅ^{-5}] and ethyl C—H [∼−23.8/∼−25.2 eÅ^{-5}] bonds, which show that the bond charges are considerably concentrated in C_{aro}—H bonds. The bond ellipticity [$\varepsilon = \lambda_1/\lambda_2$] analysis has been carried out for the study of spherical and aspherical nature of electron density at bcp. The bond charges are highly anisotropic for C_{aro}—C_{aro} [∼0.23] and charge depleted bonds C_{aro}—NO_2 [∼0.11] and N—N [N(16)—N(17); ∼0.28], whereas the ellipticity values for rest of the bonds show that the charges in the bonding regions are highly isotropic.

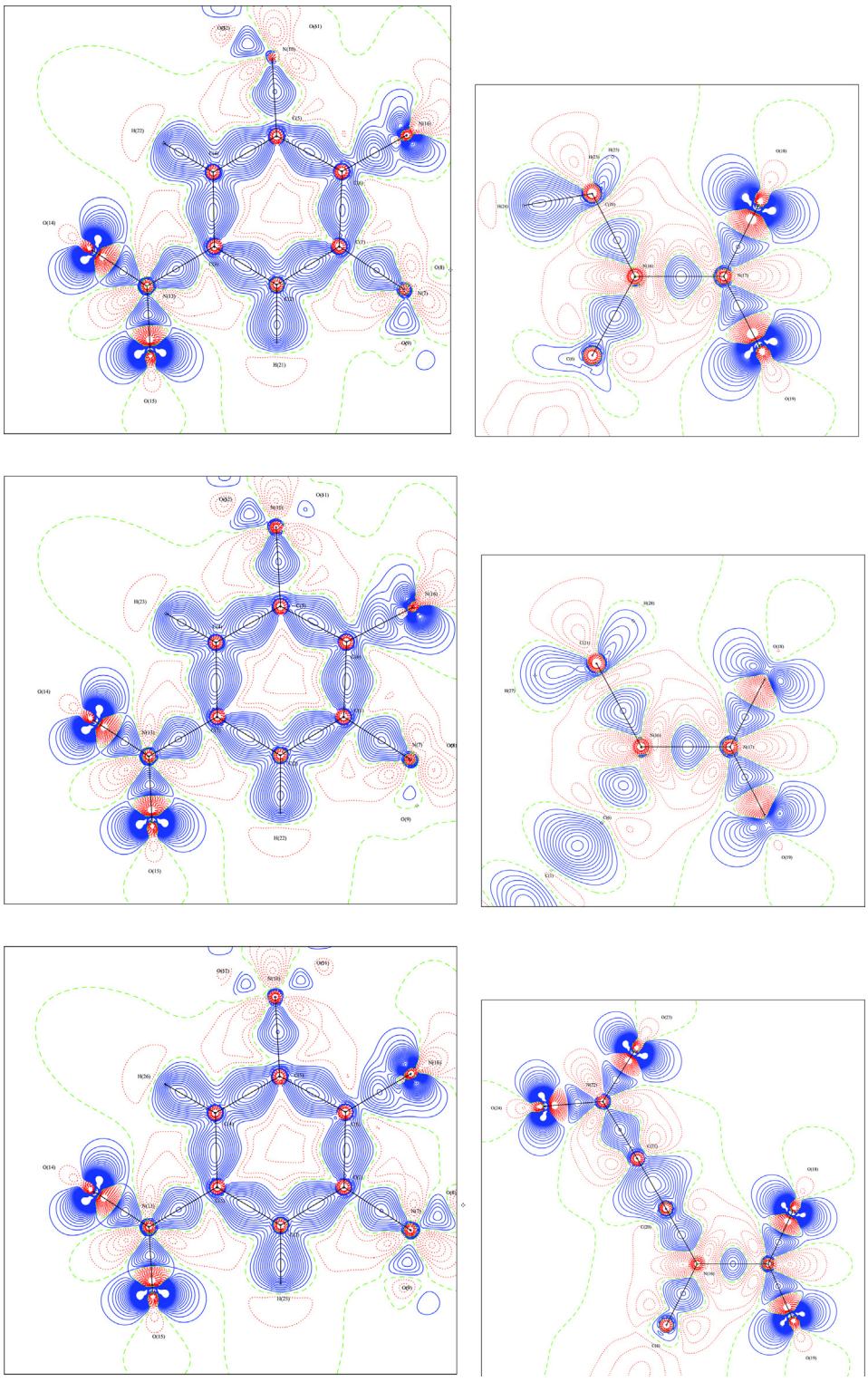

Figure 3 Deformation density maps of TNPN molecules, Blue: positive contours; Red: negative contours and the zero contours are dashed lines. The contours are drawn at 0.05 $e\text{Å}^{-3}$ intervals.

3.4. Frontier molecular orbital energies

The molecular stability is usually measured in terms of the energies of the frontier orbitals (Fukui et al., 1952). It has been characterized from the energy gap between HOMO and LUMO. The higher the energy gap, compound is much more stable and the lower energy gap implies low stability of the molecule. The energies of frontier molecular orbitals and their

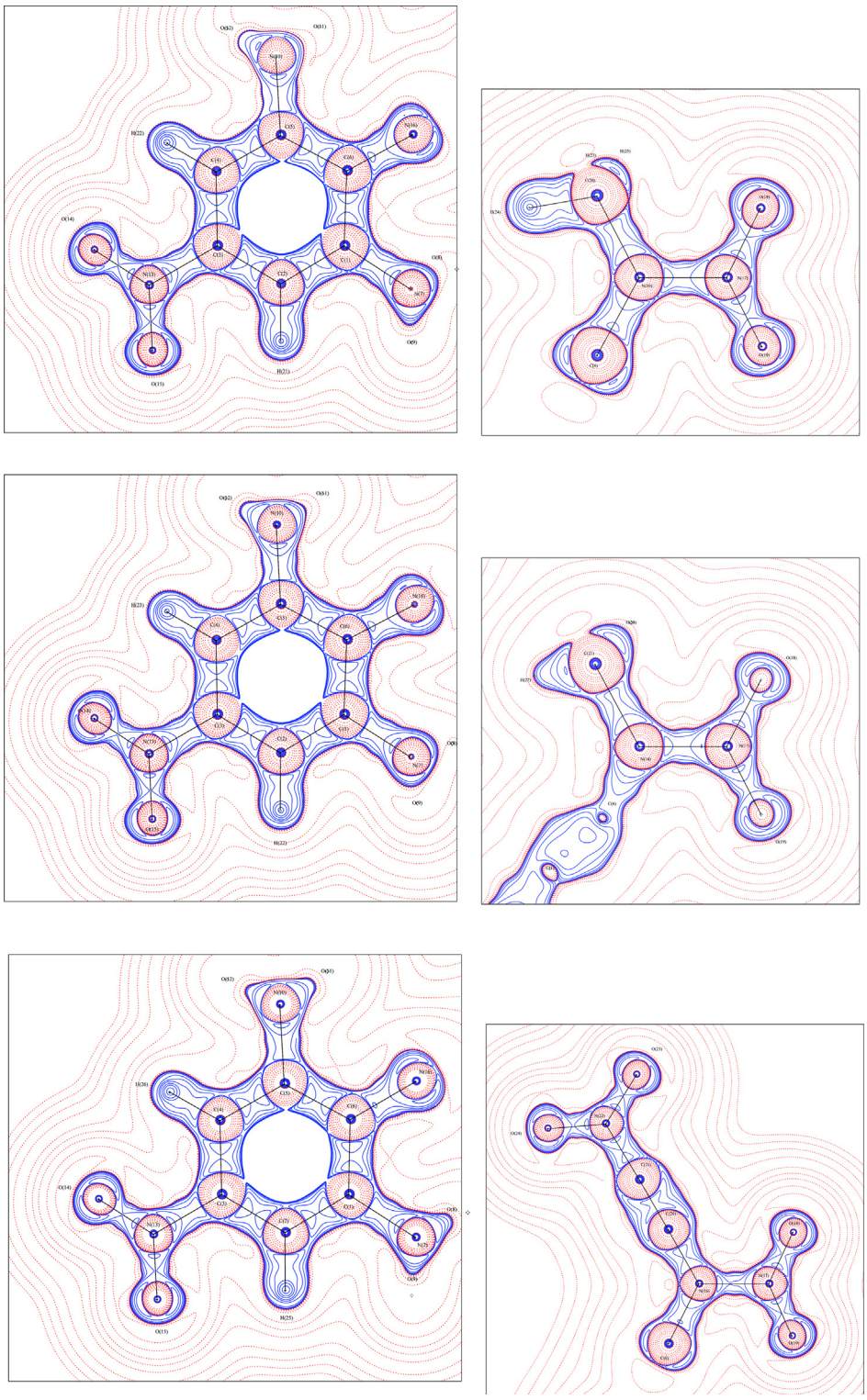

Figure 4 Plots of negative Laplacian of electron density of TNPN molecules, The contours are drawn on a logarithmic scale, 3×2^{N} eÅ^{-5}.

gaps ($\Delta E_{\text{LUMO–HOMO}}$) of MTNPN, ETNPN and NETNPN molecules were calculated at B3LYP/aug-cc-pVDZ level and are listed in Table 4. The comparative analysis of computed values of HOMO, LUMO and energy gap $\Delta E_{\text{LUMO–HOMO}}$, indicates that MTNPN and ETNPN molecules were more stable than NETNPN as their $\Delta E_{\text{LUMO–HOMO}}$ values are −4.203, −4.267 and −3.881 respectively. The $\Delta E_{\text{LUMO–HOMO}}$ values of MTNPN, ETNPN and NETNPN were found to be different, and this modification is caused by the effect of different substituents attached in C(6) atom. The effects of —NO_2

groups on HOMO and LUMO are schematically shown in Fig. 5, which display the variation of $\Delta E_{\mathrm{LUMO-HOMO}}$. As it is known, LUMO is related to molecular electron affinity, Bader's study showed that impact sensitivity of aromatic explosives will increase with decrease in LUMO energy, and so incorporation of —NO_2 group will increase sensitivity.

3.5. Oxygen balance and Impact sensitivity

Oxygen balance (OB) is one of the important properties of energetic material. It is defined as "the amount of oxygen, expressed in weight percent, liberated as a result of complete conversion of the explosive material to carbon dioxide, water, sulfur dioxide, aluminum oxide, etc." (Akhavan, 2011; Li, 2010; Owens et al., 1985). Negative oxygen balance produces greater quantity of CO and positive oxygen balance produces more NO_x gases. The equation for the oxygen balance (OB) is,

$$\mathrm{OB}_{100} = \frac{100(2n_{\mathrm{O}} - n_{\mathrm{H}} - 2n_{\mathrm{C}} - 2n_{\mathrm{COO}})}{\mathrm{M}} \tag{2}$$

where n_{O} and n_{H} represent the number of atoms of the corresponding elements in the molecule. n_{COO} is the number of carboxyl groups and M is the molecular weight. The calculated oxygen balance of MTNPN, ETNPN and NETNPN molecules ranges from −1.0448% to +0.5846% (Table 4). Interestingly, the NO_2 group increases the oxygen percentage of molecules. Further, this value has been compared with the reported explosives with high positive and negative oxygen balance (Kamlet and Adolph, 1979).

Analysis of the impact sensitivity involves dropping a weight from the variable height over the explosive sample to make 50% probability of causing an explosion (50% impact height or h_{50}) exhibiting the relation that lesser the h_{50} value higher the impact sensitivity of the molecule (Keshavarz and Jaafari, 2006). The impact sensitivity (h_{50}%) of the model compounds was calculated according to Eq. (4), from the electronic structures using charges obtained from electrostatic potential fitting methods (CHELPG) (Breneman and Wiberg, 1990) for the nitro (NO_2) groups. In nitro compounds, the C—NO_2, N—NO_2 and O—NO_2 bonds are usually the weakest bonds in the molecule, and these bonds are proven to break often at the initial steps of decomposition or detonation. The nitro group charge (Q_{NO2}) can be calculated by summing the net ESP charges of nitrogen (Q_{N}) and oxygen (Q_{O1} and Q_{O2}) atoms.

$$Q_{\mathrm{NO2}} = Q_{\mathrm{N}} + Q_{\mathrm{O1}} + Q_{\mathrm{O2}} \tag{3}$$

The higher the negative charge of NO_2 group, weaker the electron-withdrawing ability and thus the greater the overall stability of the compound. As the number of NO_2 groups in the TNPN framework increases, competition for the available charge increases and thus the molecule becomes unstable. Further, using oxygen balance and the nitro group charges (QNO_2), we have calculated the impact sensitivity, h_{50}% of MTNPN, ETNPN and NETNPN molecules. This provides a new insight into understanding the effect of molecular structure in the impact sensitivity. Studies have been reported, which evaluate the impact sensitivity of the nitro molecules which agree well within the experimental bars, by correlating the nitro group charges with impact sensitivity (Murray et al., 1995; Politzer et al., 1991). A simplified relation with much accuracy has been reported in the investigations of Cao and Gao (2007) by quantifying the nitro group charges and oxygen balance, expressed in Eq. (4) with a standard error value of 0.54 m. Regression analysis of Eq. (4) by implementing square of the nitro group charges ($Q\mathrm{NO}_2^2$) considerably reduced the standard error value to 0.19 m, which proved more accuracy with the experimental details, expressed in Eq. (5). The impact sensitivity of the molecules under concern (h_{50}%) was obtained from Eq. (5):

$$H_{50}\% = -0.2418 - 20.45Q\mathrm{NO}_2 + 0.1778\mathrm{OB}_{100} \tag{4}$$

$$H_{50}\% = 0.1926 + 98.64Q\mathrm{NO}_2^2 - 0.03405\mathrm{OB}_{100} \tag{5}$$

The predicted $H_{50\%}$ value for the MTNPN, ETNPN and NETNPN molecules is shown in Table 3, which reveals that h_{50}% values decrease as the number of NO_2 groups and other substituent group increases. This shows that the sensitivity increases from MTNPN to NETNPN. Thus inspecting the h_{50}%, Q_{NO2} and OB_{100} values, NETNPN molecule is more sensitive than MTNPN and ETNPN molecules.

3.6. Electrostatic potential and V_{mid}

The molecular electrostatic potential (MEP) explores the polarization, electron correlation, charge transfer effect and the reaction sites of the molecule (Murray et al., 2009). The molecular ESP allows identifying the electrophilic and nucleophilic sites of the molecule. Fig. 6, shows the electrostatic potential of the TNPN molecules for the isosurface values +0.5 and −0.5 eÅ^{-1}. A large electronegative region is found near NO_2 groups region, while the rest of the region is covered with positive surface. The high electronegative surface is the expected reaction surface of the molecule. This electrostatic information paves the way to predict the reaction surface of the molecule.

The sensitivities of energetic compounds are related to the anomalous charge imbalance that is characteristic of their molecular surface electrostatic potentials. There are many ways the imbalance between positive and negative surface potentials can be quantified. The balance parameters (v) can be calculated from the relation (Bulat et al., 2010).

Table 4 Oxygen balance (OB_{100}%), $\Delta E_{\mathrm{LUMO-HOMO}}$, nitro group charges ($QNO_2$) and h_{50}% of TNPN molecules at B3LYP/aug-cc-pVDZ level.

Molecule	OB_{100}%	HOMO (eV)	LUMO (eV)	$\Delta E_{\mathrm{LUMO-HOMO}}$ (eV)	QNO_2	h_{50} (m)
MTNPN	−1.0448	−8.468	−4.265	−4.203	−0.274	7.634
ETNPN	−2.3240	−8.511	−4.244	−4.267	−0.254	6.635
NETNPN	0.5846	−8.654	−4.773	−3.881	−0.255	6.587

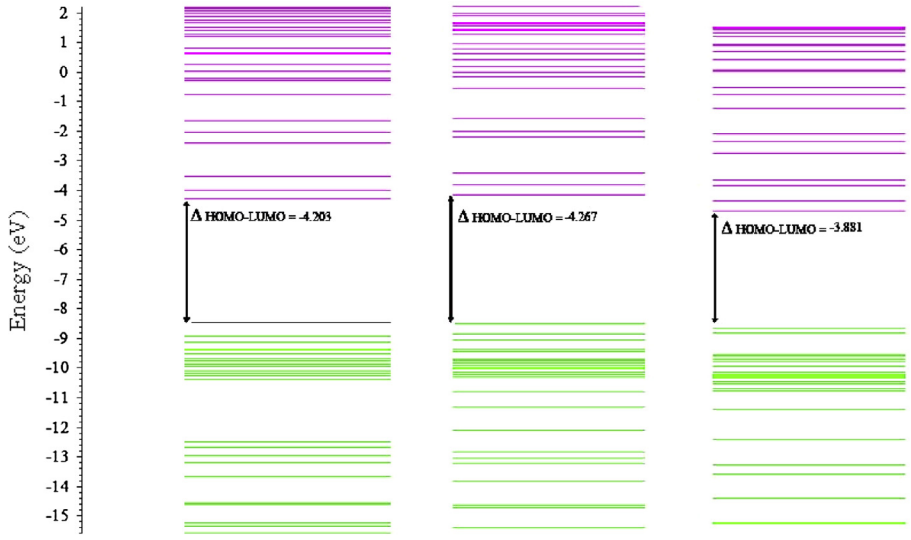

Figure 5 Energies (in eV) of frontier orbital for TNPN molecules and showing the variations of $\Delta E_{\mathrm{LUMO-HOMO}}$.

$$v = \frac{\sigma_+^2 \sigma_-^2}{\left(\sigma_+^2 + \sigma_-^2\right)^2} \tag{6}$$

The quantities σ_+^2 and σ_-^2 are the indicators of the strengths and variability of positive and negative surface potentials. The degree of balance between the positive and negative surface potentials is measured by v. The balance parameter v reaches a maximum value 0.25, when $\sigma_+^2 = \sigma_-^2$. Here, we have calculated the positive and negative electrostatic potential variances (σ_+^2 and σ_-^2) and the electrostatic balance parameter (ν) of TNPN molecule from DFT method, and the corresponding values are shown in Table 5. The sensitivity of NETNPN molecule is further empathized from its highest σ_+^2 [176.60] values among the rest of the molecules.

The most notable feature of the electrostatic potential of energetic molecule is its important relation with the impact sensitivity. Here, we explore the concept proposed by Murray et al. (2009) regarding the buildup of positive ESP over C—NO_2 bonding region and to relate its impact sensitivity. To correlate the ESP with the impact sensitivity, we investigated the electrostatic potential V_{mid} at the bond mid points of the molecule, which is defined as

$$V_{mid} = \frac{Q_i}{0.5R} + \frac{Q_j}{0.5R} \tag{7}$$

where Q_i and Q_j are the atomic charges of ith and jth atoms, and R is the bond distance. Here, we investigate the concept proposed for the V_{mid} calculation (Table 5) for the charges obtained from CHELPG model to relate to the bond charge depletion. Interestingly, the calculation of V_{mid} for all C—N bonds emphasizes that the highly charge depleted bonds C(1)—N(7), C(3)—N(13), C(5)—N(10) and N(16)—N(17) are the sensitive bonds, which is confirmed from the calculated high positive V_{mid} values as shown in Table 5. Thus the V_{mid} result confirms that C—NO_2 and N—N bonds are the weakest and highly sensitive bonds toward the external shock.

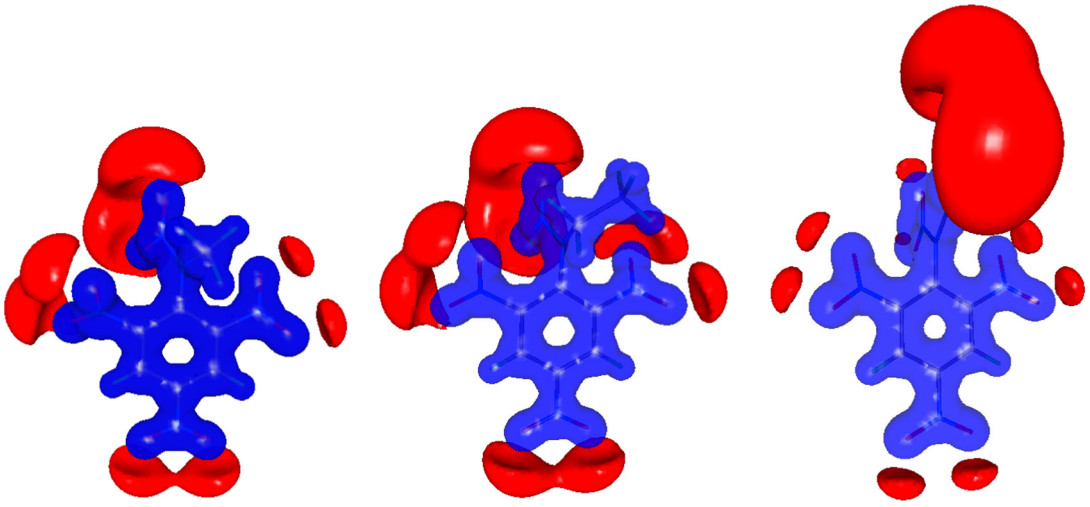

Figure 6 Isosurface representation of electrostatic potential of TNPN molecules, Blue: positive potential ($+0.5$ eÅ^{-1}) and Red: negative potential (-0.5 eÅ^{-1}).

Table 5 Electrostatic potential at the bond mid points V_{mid} ($e\text{Å}^{-1}$) and imbalance parameters of TNPN molecules calculated from ESP model charges.

Bonds	MTNPN	ETNPN	NETNPN
C(1)—C(2)	−0.20	−0.27	−0.13
C(2)—C(3)	−0.08	−0.05	−0.01
C(3)—C(4)	0.00	−0.01	−0.01
C(4)—C(5)	−0.12	−0.18	−0.13
C(5)—C(6)	0.09	0.20	0.05
C(6)—C(1)	0.09	0.15	0.04
C(6)—N(16)	−0.04	−0.10	0.23
C(1)—N(7)	0.99	0.97	0.90
C(5)—N(10)	0.93	0.91	0.90
C(3)—N(13)	0.97	0.97	0.92
N(7)—O(8)	0.51	0.58	0.47
N(7)—O(9)	0.52	0.56	0.48
N(10)—O(11)	0.43	0.43	0.47
N(10)—O(12)	0.51	0.54	0.48
N(13)—O(14)	0.40	0.39	0.40
N(13)—O(15)	0.39	0.38	0.40
N(16)—N(17)	0.98	0.81	1.19
N(17)—O(18)	0.57	0.60	0.68
N(17)—O(19)	0.51	0.54	0.59
N(16)—C(20)	−0.31	0.08	0.13
σ_+^2	110.63	107.31	176.6
σ_-^2	32.35	33.62	34.74
v	0.18	0.18	0.14

4. Conclusion

The bond topological and the electrostatic properties of TNPN molecule and its derivatives have been carried out to recognize their bond strengths, and to analyze the relation between the strength of the bond and impact sensitivity using high level quantum chemical calculations and Bader's atoms in molecules analysis. Geometrical studies from DFT [B3LYP] method revealed the consistency of the parameters of the molecules for both polarized and augmented basis sets of 6-311G** and aug-cc-pVDZ respectively. Topological studies to analyze the Laplacian and electron density exposed maximum electron charge density over N-O bonds, revealing their highly concentrated covalent bonding nature with high negative values. The studies also revealed that the C—NO_2 bonds were exhibiting significantly low Laplacian and electron density values (−16.1 $e\text{Å}^{-5}$/1.74 $e\text{Å}^{-3}$), conforming the bonds are depleted and sensitive to external shocks. Aside from C—NO_2 bonds, the N(16)—N(17) bond of the NETNPN was found to be highly depleted (−5.9 $e\text{Å}^{-5}$) and the weakest bond among the three candidates with its corresponding low energy density [$H(r)$]. The research explored that the presence of additional functional groups affects the charge accumulation on a molecule, where the expanded charge density over C(20)—C(16) of NETNPN is due to the —$CCNO_2$ attachment with C(20) atom. The impact sensitivity and oxygen balance parameter for TNPN and its derivative molecules were evaluated from the calculated net electrostatic potential charges of nitro groups, and exposed NETNPN molecule is likely to be more sensitive than the other molecules, exhibiting positive value of oxygen balance (0.5846) and low H_{50}% of 6.587 m. The V_{mid} calculations from the electrostatic potential at the midpoint of the existing bonds of the molecules also confirmed that C—NO_2 and N—N bonds are more sensitive to external shocks, and rupture quickly than the other bonds by indicating high positive values. The less stability and higher impact sensitivity of the NETNPN molecule can also be authenticated from the lesser energy gap between the frontier orbitals ($\Delta E_{LUMO\text{-}HOMO}$ = −3.881 eV). Therefore we conclude that depleted C—NO_2 and N—N bonds are the most sensitive bonds evaluated from the three TNPN structures, in which NETNPN molecule being the most sensitive to external shocks.

Acknowledgment

The authors were grateful to the DST-SERB for providing financial assistance and support in the proper completion of the research. Authors are also grateful to the CDAC-Bangalore cluster computing facilities for the computational aid provided throughout the research work.

References

Agarwal, J.P., 2011. High Energy Materials. Wiley-VCH, Weinheim.
Akhavan, J., 2011. The Chemistry of Explosives. The Royal Society of Chemistry.
Anders, G., Borges, I., 2011. Topological analysis of the molecular charge density and impact sensitivity models of energetic molecules. J. Phys. Chem. A 115, 9055–9068.
Bader, R.F., 1990. Atoms in Molecules. Wiley Online Library.
Bader, R.F.W., Nguyen-Dang, T.T., Tal, Y., 1981. A topological theory of molecular structure. Rep. Prog. Phys. 44.
Biegler-könig, F.W., Bader, R.F.W., Tang, T.-H., 1982. Calculation of the average properties of atoms in molecules. II. J. Comput. Chem. 3, 317–328.
Breneman, C.M., Wiberg, K.B., 1990. Determining atom-centered monopoles from molecular electrostatic potentials. The need for high sampling density in formamide conformational analysis. J. Comput. Chem., 361–373
Brovarets, O.H.O., Hovorun, D.M., 2013. Atomistic understanding of the C·T mismatched DNA base pair tautomerization via the DPT: QM and QTAIM computational approaches. J. Comput. Chem. 34, 2577–2590.
Bulat, F.A., Toro-Labbé, A., Brinck, T., Murray, J.S., Politzer, P., 2010. Quantitative analysis of molecular surfaces: areas, volumes, electrostatic potentials and average local ionization energies. J. Mol. Model. 16, 1679–1691.
Butcher, R.J., Bottaro, J.C., Gilardi, R., 2003. 1,3,4-Trinitro-7,8-diazapentalene. Acta Crystallogr. Sect. E 59, o1780–o1782.
Cao, C., Gao, S., 2007. Two dominant factors influencing the impact sensitivities of nitrobenzenes and saturated nitro compounds. J. Phys. Chem. B 111, 12399–12402.
Cooper, P.W., 1996. Explosives Engineering. Wiley-VCH, New York.
Frish, A., Leen, E., Nielson, A.B., Holder, A.J., Dennigton, Roy D., Keith, T.A., 2005. Gaussian Incorporated, Pittsburgh PA.
Fukui, K., Yonezawa, T., Shingu, H., 1952. A molecular orbital theory of reactivity in aromatic hydrocarbons. J. Chem. Phys. 20, 722–725.
Hanwell, M.D., Curtis, D.E., Lonie, D.C., Vandermeersch, T., Zurek, E., Hutchison, R., 2012. J. Cheminf. 4, 17.
Hübschle, C.B., Luger, P., 2006. MolIso – a program for colour-mapped iso-surfaces. J. Appl. Crystallogr. 39, 901–904.
Kamlet, M., Adolph, H., 1979. The relationship of impact sensitivity with structure of organic high explosives. II. Polynitroaromatic explosives. Propellants, Explos., Pyrotech. 4, 30–34.
Keshavarz, M.H., Jaafari, M., 2006. Investigation of the various structure parameters for predicting impact sensitivity of energetic molecules via artificial neural network. Propellants, Explos., Pyrotech. 31, 216–225.
Klapötke, T.M., 2011. Chemistry of High-Energy Materials. Wdeg, Berlin.
Koritsanszky, T., Macchi, P., Gatti, C., Farrugia, L.J., Mallinson, P. R., Volkov, A., Richter, T., 2007. XD-2006, a computer program package for multipole refinement and topological analysis of charge densities and evaluation of intermolecular energies from experimental or theoretical structure factors, version 5.33.

Li, J., 2010. Relationships for the impact sensitivities of energetic C-nitro compounds based on bond dissociation energy. J. Phys. Chem. B 114, 2198–2202.

Lide, D.R., 1967. A survey of carbon-carbon bond lengths. Tetrahedron 17, 125–134.

Murray, J.S., Concha, M.C., Politzer, P., 2009. Links between surface electrostatic potentials of energetic molecules, impact sensitivities and C–NO_2/N–NO_2 bond dissociation energies. Mol. Phys. 107, 89–97.

Murray, J.S., Lane, P., Politzer, P., 1995. Relationships between impact sensitivities and molecular surface electrostatic potentials of nitroaromatic and nitroheterocyclic molecules. Mol. Phys. 85, 1–8.

Owens, F.J., Jayasuriya, K., Abrahmsen, L., Politzer, P., 1985. Computational analysis of some properties associated with the nitro groups in polynitroaromatic molecules. Chem. Phys. Lett. 116, 434–438.

Politzer, P., Murray, J.S., Lane, P., Sjoberg, P., Adolph, H.G., 1991. Shock-sensitivity relationships for nitramines and nitroaliphatics. Chem. Phys. Lett. 181, 78–82.

Perdew, J.P., 1986. Density-functional approximation for the correlation energy of the inhomogeneous electron gas. Phys. Rev. B 33, 8822–8824.

Stephen, A.D., Thomas, R., Srinivasan, P., Narayayanasamy, V., Kumaradhas, P., 2011. Exploring the bond topological and electrostatic properties of benzimidazole molecule via experimental and theoretical charge density study. J. Mol. Struct. 989, 122–130.

Stephen, A.D., Pawar, R.B., Kumaradhas, P., 2010. Exploring the bond topological properties and the charge depletion-impact sensitivity relationship of high energetic TNT molecule via theoretical charge density analysis. J. Mol. Struct. (THOECHEM) 959, 55–61.

Sutton, L.E., 1965. Tables of Interatomic Distances. The Chemical Society, London.

Zhang, C., 2008. Investigation of the correlations between nitro group charges and some properties of nitro organic compounds. Propellants, Explos., Pyrotech. 33, 139–145.

Zhang, C., 2009. Review of the establishment of nitro group charge method and its applications. J. Hazard. Mater. 161, 21–28.